

Object-based binary encoding algorithm -an integration of hyperspectral data and DSM

Huan Xie, Xiaohua Tong
Department of Surveying and Geo-informatics
Tongji University
1239 Siping Road, Shanghai, 200092, China
xiehuantj@gmail.com

Christian Heipke, Peter Lohmann, Uwe Sörgel
Institut für Photogrammetrie und GeoInformation
Leibniz Universität Hannover
Nienburger Str. 1, D-30167 Hannover, Germany

Abstract—The advent of advanced processing techniques and high speed computers have led to the possibility of supplementary hyperspectral data with information about different kinds of object features that can be observed in the images, for example, shape and size. Other data sources, *e.g.*, digital surface model from airborne laser scanning data, can provide height information for the object features. In this paper an improved binary encoding method (IBE) is proposed to integrate such additional information into the binary encoding matching method. The original binary encoding method proceeded spectral information pixel by pixel; IBE method is based on object-based classification. The hyperspectral and DSM data were corporately used in the method. During the method, the information of target objects was represented by 280 binary codes according to IBE rules, practical experiences and user requirements. We applied the proposed method to classify the test area. The results show that the proposed method needs less training data, lower computation cost and can gain higher classification accuracy. It is beneficial especially for limited spatial extent and great variation of the ground contents.

Keywords- Hyperspectral, DSM, binary encoding, object-based classification

I. INTRODUCTION

In principle, standard classification algorithms designed for multispectral imagery can be directly applied to hyperspectral data, because no theoretical limitations on the number of bands (of features) exist. However, in practice algorithms such as Maximum-Likelihood (ML), even with efficiency improvements (Bolstad and Lillesand, 1991; Jia and Richards, 1993; Lee and Landgrebe, 1991), tend to perform poor when applied to hyperspectral image of 200 bands. Furthermore, in case of ML the parameters class mean vectors and covariance matrixes have to be estimated, assuming Gaussian class. If K spectral or other features are used, the training set for each class must contain at least $K+1$ pixels in order to calculate the sample covariance matrix. To obtain reliable class statistics, 10 to 100 training pixels per class, per feature are typically needed (Swain and Davis, 1978). These conditions may be impossible to meet for some classes of limited spatial extent. Therefore, a number of special, non-parametric classification tools have been developed tailored for hyperspectral imagery. Their structure is not only driven by a need for efficiency, but also by

different types of pattern recognition made possible by the high-resolution spectral data.

Binary spectral encoding is well known as a simple, effective, and with small computational load hyperspectral analysis method in classification, searching of similar spectra and identifying mineral components (Mazer *et al.*, 1988). Although this method is frequently used and offers good performance, it still can be improved. Due to the high spatial resolution of modern hyperspectral sensors and because this method mainly operates on pixels, the efficiency sometimes is low. Nowadays, with the rapid development of advanced remote sensor technologies with increasing spatial resolution, object-based data processing methods are more frequently applied. This paper therefore attempts to integrate an object-based approach with traditional hyperspectral processing methods to support and enhance the information extraction from remote sensing data.

Several processing are carried out. First segments have to be established. In this paper, an edge-based segmentation algorithm and the Full Lambda-Schedule algorithm (Robinson *et al.*, 2002) are employed to partition the data spatially and merge adjacent segments, respectively. The mean spectrum of all pixels belonging to the segment is chosen as representative spectrum. The most important task then is, to find a way to integrate shape and height information with binary coding, like it is done with the spectral information. Several shape description measures, *e.g.*, area, compactness, will be discussed.

Following this introduction, a short description of the study area is given. Then data processing and binary encoding methods proposed in this paper are described, especially the binary coding representation of different kinds of features (spectral, shape and height information) and the computation of the signature distances. Practical tests, illustrating the proposed methods are presented and finally some conclusions are drawn at the end.

II. METHODS

A. Study area

The study area Oberpfaffenhofen is located in the south of Germany. The available digital surface model of this region has a spatial spacing of 0.5 meters. The Hymap data of this area

was captured at 13:00, June 7, 2004 at a flight altitude of 2580 meters above sea level, and a flight direction from south to north (3.6°). This data have a ground resolution of 4 meters and 126 channels. Technical details of the HyMap sensor can be found in Cocks *et al.* (2001).

B. Flow chart

Figure 1 shows the overall flowchart of the project. Several pre-processing procedures for Hymap image and DSM data are performed, e.g., the geometric and atmospheric correction of Hymap images and the detection of ground objects from DSM data. The DSM represents elevated objects, such as buildings, in contrast the DEM as defined here follows the terrain. Afterwards, segments are established using HyMap image by an edge-based segmentation algorithm. Second, the mean spectrum was selected as the representative spectrum of the segment. After that, 5 shape descriptors are calculated for each segments and transformed to binary codes: area, asymmetry, rectangular fit, the ratio of length to width, and compactness. The relative heights derived from DSM were converted to binary codes too. After the encoding for all segments, according to practical experiences and users' requirements, corresponding codes for 14 categories are set up. The segments are then classified to different categories according to their similarities with these categories.

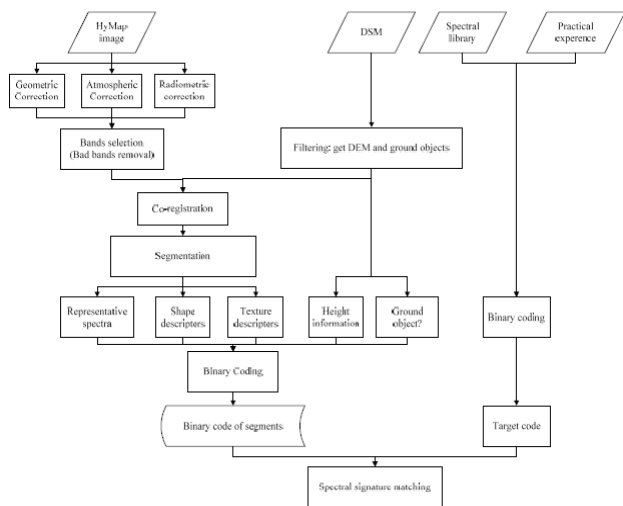


Figure 1. Flow Chart

C. Segmentation

A segmentation algorithm is used with the expectation that it will divide the image into semantically significant regions, or objects, to be recognized by further processing steps. Several segmentation approaches have been proposed, e.g., Le Moigne and Tilton (1995), Kartikeyan *et al.* (1998), Acharyya *et al.* (2003), Duarte-Carvajalino *et al.* (2008), and comparisons are made to evaluate the quality of segmentation (Trias-Sanz *et al.*, 2008). Due to that the segmentation is not the research focus of the paper, based on visual interpretation, an edge based segmentation and merging algorithm was applied. This algorithm iteratively merges adjacent segments based on a combination of spectral and spatial information. Merging

proceeds if the algorithm finds a pair of adjacent regions, i and j , such that merging cost $t_{i,j}$ is less than a defined threshold lambda value, which ranges from 0.0 to 100.0:

$$t_{i,j} = \frac{|O_i| \cdot |O_j| \cdot \|u_i - u_j\|^2}{(|O_i| + |O_j|) \cdot \text{length}(\partial(O_i, O_j))} < \lambda \quad (1)$$

Where O_i is region i of the image, $|O_i|$ is the area of region i , u_i is the pixel mean value in region i , u_j is the pixel mean value in region j , $\|u_i - u_j\|$ is the Euclidean distance between the spectral values of regions i and j , $\text{length}(\partial(O_i, O_j))$ is the length of the common boundary of O_i and O_j , the lambda value we chose here is 88.0.

D. Binary encoding for segments

The binary code of an image object in our research is constructed by a 280-bit long code, which consists of three parts, i.e., spectrum, shape and size, and height. The spectral amplitude and slope are represented by 252 codes \overline{Y}_{ij} , the shape and size of the segment is represented by 25 codes \overline{Z}_{ij} , and the relative height of a segment is represented by 3 codes. Specific explanations for these codes can be found in following contents.

1) Spectrum

According to Mazer *et al.* (1988), layer mean values are calculated from the layer values of all n pixels forming an image object. In spectral binary encoding method, a single spatial resolution element of the image (pixel) is denoted by an L -dimensional vector,

$$\overline{X}_{ij} = [X_{ij}(1), X_{ij}(2), \dots, X_{ij}(L), \dots, X_{ij}(L)]^T \quad (2)$$

where L is the number of spectral channels, and the indices (i, j) refer to the spatial location of the pixel within a given scene. Defining the scalar quantity v_{ij} as the spectral mean of pixel (i, j) ,

$$v_{ij} = \left[\frac{1}{L} \right] \sum_{l=1}^L X_{ij}(l) \quad (3)$$

an L -bit binary code vector \overline{Y}_{ij}^a is constructed from

$$\overline{Y}_{ij}^a = H \{ \overline{X}_{ij} - v_{ij} \} \quad (4)$$

where $H(v)$ is the unit step operator defined by

$$H(v) = \begin{cases} 0, & v \geq 0 \\ 1, & v < 0 \end{cases} \quad (5)$$

The constructed vector is a binary representation of spectral amplitude; however, considerable information is contained in the local slope at each measured wavelength. Therefore, an additional L -bit code vector \overline{Y}_{ij}^b is constructed from

$$\overline{Y_{ij}^b} = \begin{cases} 0, & [X_{ij}(l+1) - X_{ij}(l-1)] < 0 \\ 1, & [X_{ij}(l+1) - X_{ij}(l-1)] \geq 0 \end{cases}, l = 1, 2, \dots, L \quad (6)$$

Here $X_{ij}(0) = X_{ij}(0), X_{ij}(L+1) = X_{ij}(1)$, these two code vectors $\overline{Y_{ij}^a}$ and $\overline{Y_{ij}^b}$ are then concatenated to form a single, $2L$ -bit code vector $\overline{Y_{ij}}$, which is taken to be the binary code word representing the spectrum of pixel (i, j) .

The calculation for the spectral binary codes was realized by IDL/ENVI programming.

2) Shape

The value of shape and size attributes can be either computed by professional software, e.g., eCognition, or collected by IDL/ENVI programmes. The shape and size attributes of a segment are represented by 25 codes, including the information of area, asymmetry, compactness, rectangular_fit, and the ratio of length to width.

a) Area

In nongeoreferenced data, the area of a single pixel is 1. Consequently, the area A of an image object is the number of pixels forming it. If the image data is georeferenced, the area of an image object is the true area covered by one pixel times the number of pixels forming the image objects.

b) Asymmetry

The lengthier an image object, the more asymmetric it is. For an image object, an ellipse is approximated, and the asymmetry is expressed by the ratio of the length of minor axis n and the length of major axis m of this ellipse.

$$Asymmetry = 1 - \frac{n}{m} \quad (7)$$

The feature value increases with the asymmetry, and the asymmetry value for a segment ranges from zero to one.

c) Compactness

Compactness here is defined as the ratio of the area A_p of a polygon to the area of a circle with the same perimeter. The following formula is used to calculate the compactness of the selected polygon. The compactness of a segment ranges from zero to one and a circle has the highest compactness value.

$$Compactness = \frac{4 \cdot \pi \cdot A_p}{Perimeter^2} \quad (8)$$

in which, the *Perimeter* is the sum of the lengths of all edges which form the polygon of the image object. The computation of base polygons is done by means of a Douglas Peucker algorithm which is one of the most common procedures for polygon extraction. It is a top-down approach, which starts with a given polygon line and divides it into smaller sections iteratively.

d) Rectangular fit

A first step in the calculation of the rectangular fit is the creation of a rectangle with the same area as the considered object. In the calculation of the rectangle also the proportion of the length to the width of the object is regarded. After this step

the area of the object outside the rectangle A_o is compared with the area A covered by the image object. While 0 means no fit, 1 stands for a complete fitting object.

$$RectangularFit = 1 - \frac{A_o}{A} \quad (9)$$

e) Length/width ratio

There are two ways to compute the length/width ratio of an image object.

The ratio length/width is identical to the ratio of the eigenvalues of the covariance matrix of the image object with the larger eigenvalue being the numerator of the fraction.

$$\gamma = \frac{l}{w} = \frac{eig_1(S)}{eig_2(S)}, eig_1(S) > eig_2(S) \quad (10)$$

Or the ratio length/width can also be approximated using the bounding box.

$$\gamma = \frac{l}{w} = \frac{a^2 + ((1-f) \cdot b)^2}{A} \quad (11)$$

a is the length of the bounding box of the segment, b is the width of the bounding box, f is the degree of filling, which is the area A covered by the image object divided by the total area $a * b$ of the bounding box.

We use both methods for the calculation and takes the smaller of both results as the feature value. The minimum value of the Length/width is 1. The encoding for these descriptors follows the same way, each descriptor is represented by 5 binary codes. Take descriptor Area for example, the areas of the segments in our study area ranges from 16 square meters to 1162000 square meters (from 1 to 72625 pixels), according to the histogram of the areas of the segments. We separate the segments into 5 cases by their histogram bins. Each case covers approximately 20 percent of the histogram area, as we can see in Figure 2. Then the areas of the segments are represented by 5 codes. Such as 00100, means the area of this segment is greater than T2 and less than T3.

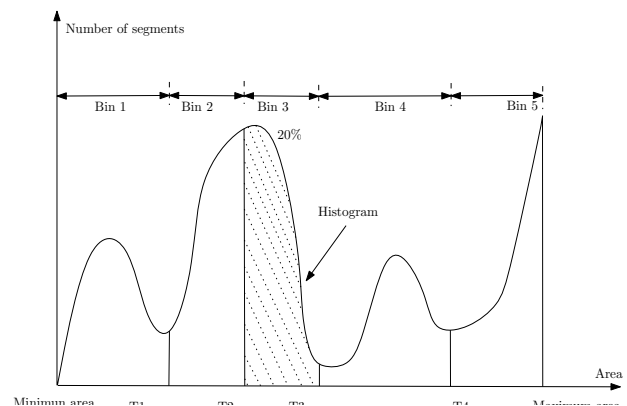


Figure 2. The encoding rule for Area

The values of shape descriptors were calculated using Definiens eCognition and ESRI's ArcGIS software. The

binary encoding for those shape descriptors were realized by IDL/ENVI programming.

3) Height

The height information can be obtained from the stereo images or other height information sources, e.g., airborne laser scanning (Lidar), Synthetic-aperture radar (SAR) data. We used the relative height information of the ground object in the paper. The DTM was first filtered from the DSM data, then the relative heights of image objects were derived from the difference between DTM and DSM.

The binary codes of height are determined by the relative height of image objects. According to the practical experiences, we separate the image objects into three cases: height less than 1.5 meters, height greater than 1.5 meters but less than 5 meters, and height greater than 5 meters. Code '001' means that the relative height of the image object is greater than 5 meters.

E. Target Codes

According to the actually land use and land cover of our study area, several codes for certain targets have been set up. Referenced the Land use and land cover categories raised by USGS (Anderson *et al.*, 1976), we selected the classes Residential buildings, Industrial and other buildings, Mixed urban areas, Roads, Vacant, Cropland, Tree mixed grass, and Tree. More classes, especially different types of cropland, can be set up following in-situ measurements and investigations. Corresponding codes were created for every target for further signature matching.

TABLE I. THE CLASSIFICATION TARGETS AND THEIR FEATURES

Classes	Number of spectral samples	Bin(s) of histogram				
		Shape				Height
		Area	Asymmetry	Compactness	Length/width	Rectangular Fit
Residential buildings	5	1-2	1-2	3-5	1-3	2-3
Industrial and other buildings	15	2-5		3-5	1-4	3-5
Mixed urban areas	12			1-3		1-2
Roads	9	1-3	4-5	1-2	5	1
Vacant	4	1-3	1-3	3-5	1-3	3-5
Cropland1	7	2-5	1-4	3-5	1-4	3-5
Cropland2	4	2-5	1-4	3-5	1-4	3-5
Cropland3	4	2-5	1-4	3-5	1-4	3-5
Cropland4	5	2-5	1-4	3-5	1-4	3-5
Cropland5	2	2-5	1-4	3-5	1-4	3-5
Tree mixed grass	4	1-3		1-3	1-3	1-3
Tree	7	1-3		1-3	1-3	1-3
Other 1	2	1-3	3-5		1-3	3-5
Other 2	1					1-2

Several assumptions have been met before coding certain targets, which will be verified by in-situ investigation in future. These assumptions are: The residential buildings generally have a uniform size and spacing, and the areas and heights of residential buildings are comparably smaller than those of industrial buildings. The industrial, commercial and other buildings are more likely to have different sizes. The spectrum

of the building varies depending on the materials and the vegetation cover of the roof.

Roads have similar spectrum like Vacant. The Roads and Vacant are separated by the shape and the ratio of length to width. Cropland is classified into several categories according to its status. Unnamed classes, other1 and other2, are added to the category list according to their distinguished spectral characteristics, their actually land use and land cover type will be specified in the further studies.

The principles of setting the target code are listed in Table 1. Column 1 lists the Land use/ Land cover type we used in our test. Column 2 lists the corresponding number of spectral samples. Column 3 to 7 lists the requirements for shape descriptors. Column 8 lists the properties of height. Blanks in column 3 to 7 mean that there are no corresponding requirements for this attribute.

The spectral binary codes of targets were represented by 2*126 bit long codes, following the same way with the segment encoding.

Comparing to the codes of spectrum, the codes for the shape and height of targets are handled in a different way. Take the area of Roads for example, the area of Roads ranged from Area1 to Area 3, the binary code for the area of Roads is 11100. The binary code for the blanks in column 3 to 8 is 11111.

F. Signature matching

The similarity measure used to determine spectral signature matches is the Hamming distance (Viterbi and Omura, 1979), which is computed from

$$D_h(\bar{Y}_{ij}, \bar{Y}_{mn}) = \sum_{l=1}^{2L} Y_{ij}(l)(XOR)Y_{mn}(l) \quad (12)$$

which is seen to be just a 2L sum of bit-wise exclusive-OR operations. In the actual implementation of this algorithm, Hamming distances D_h^a and D_h^b are computed separately for the two components of the vectors \bar{Y}_{ij} and \bar{Y}_{mn} which are being compared. This gives the user some additional flexibility in weighting the importance of amplitude and slope information.

Different from the spectral data, the operator used in the similarity evaluation of shape and height descriptors is the bit-wise AND operation, which is computed from

$$D_h(\bar{Z}_{ij}, \bar{Z}_{mn}) = 6 - \sum_{l=1}^{28} Z_{ij}(l)(AND)Z_{mn}(l) \quad (13)$$

This distance is more like a mask operation. For one descriptor, only 1 (matched) or 0 (unmatched) will be shown in the results of calculation.

The distances of spectrum, shape and height were added up to determine the distance to the targets. Since perfect matches rarely occur with real data, allowance for natural variability is made by specifying a threshold distance of acceptance. Or, if no threshold is set and several target classes are given, the minimum distance between the segment and all class targets is

chosen as the distance of acceptance of this segment. For one segment, the distance with all samples will first be calculated and the minimum distance i and the class j with the minimum distance will be recorded. If the distance i is less than the threshold, the segment will be assign to class j , or the segment will be assign to the class "Unclassified".

III. RESULTS

To compare the classification results, binary encoding classification were used on the raw HyMap data and the segment regional mean of Hymap. Figure 3 shows the comparison of classification. Figure 3(a) shows the classification result using our improved binary encoding method, Figure 3(b) shows the ordinary binary encoding classification result using the Hymap image.

From Figure 3, we can found that the traditional binary encoding method can hardly tell the differences between road, vacant and building, see Figure 3(b).However, with the help of length to width ratio, and the help of height information, the method proposed by this paper classified almost roads into the right class, as we can see in Figure 3(a).

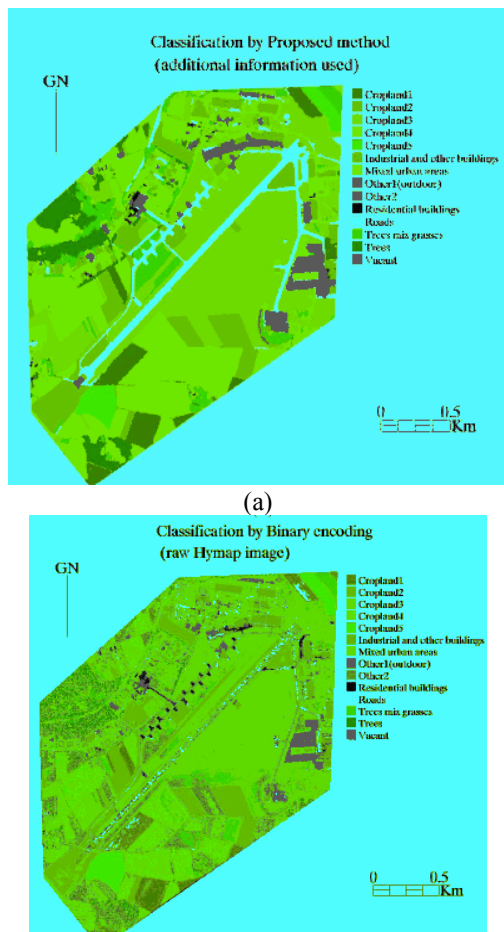


Figure 3. The classification results by binary encoding and our proposed method

According the error matrixes resulting from classifying training set of these classifications. We can found that the overall accuracy of our proposed method can be reach to 95%, while the overall accuracy of the binary encoding classification is only 68%. Due to that object-based classification technique is used, the error matrixes are calculated from the number of training set segments instead of the number of training set pixels. Table2 listed the error matrix resulting from classifying training set segments of the proposed method.

TABLE II. ERROR MATRIX RESULTING FROM PROPOSED METHOD BY CLASSIFYING TRAINING SET SEGMENTS

	Training Set Data ^a														Row Total
	C1	C2	C3	C4	C5	IB	MU	O1	O2	RB	R	TM	T	V	
Classification Data															
C1	7	0	0	0	0	0	0	0	0	0	0	0	0	0	7
C2	0	4	0	0	0	0	0	0	0	0	0	0	0	0	4
C3	0	0	4	0	0	0	0	0	0	0	0	1	0	0	5
C4	0	0	0	5	0	0	0	0	0	0	0	0	2	0	7
C5	0	0	0	0	2	0	0	0	0	0	0	0	0	0	2
IB	0	0	0	0	0	15	0	0	0	0	0	0	0	0	15
MU	0	0	0	0	0	0	12	0	0	1	0	0	0	0	13
O1	0	0	0	0	0	0	0	2	0	0	0	0	0	0	2
O2	0	0	0	0	0	0	0	0	1	0	0	0	0	0	1
RB	0	0	0	0	0	0	0	0	0	4	0	0	0	0	4
R	0	0	0	0	0	0	0	0	0	0	8	0	0	0	8
TM	0	0	0	0	0	0	0	0	0	0	0	4	0	0	4
T	0	0	0	0	0	0	0	0	0	0	0	0	4	0	4
V	0	0	0	0	0	0	0	0	0	0	0	0	0	4	4
Column Total	7	4	4	5	2	15	12	2	1	5	9	4	6	4	80
Producer's Accuracy															
Cropland1						100.00%	User's Accuracy					Cropland1	100.00%		
Cropland2						100.00%	Cropland2					100.00%			
Cropland3						100.00%	Cropland3					80.00%			
Cropland4						100.00%	Cropland4					71.43%			
Cropland5						100.00%	Cropland5					100.00%			
Industrial and other buildings						100.00%	Industrial and other buildings					100.00%			
Mixed urban areas						100.00%	Mixed urban areas					92.31%			
Other1						100.00%	Other1					100.00%			
Other2						100.00%	Other2					100.00%			
Residential buildings						80.00%	Residential buildings					100.00%			
Roads						88.89%	Roads					100.00%			
Trees mix grasses						100.00%	Trees mix grasses					100.00%			
Trees						66.67%	T rees					100.00%			
Vacant						100.00%	Vacant					100.00%			
Overall Accuracy=95%															

^aC1, cropland 1; C2, cropland 2; C3, cropland 3; C4, cropland 4; C5, cropland 5; IB, industrial and other buildings; MU, mixed urban areas; O1, other 1; O2, other 2; RB, residential buildings; R, roads; S, schools; TM, trees mixed areas; T, trees; V, vacant

IV. CONCLUSIONS

Based on the idea that integrating multi-sources remote sensing data may improve the interpretation of remote sensing data, a rough improved binary encoding classification method was presented. This method changes the pixel-based classification to object (segment) based classification and added the shape and the height information of segments into the codes of the segments. The classification results show that our method has advantages in the classification of similar spectral objects and retains the characteristics of the ordinary binary encoding method. More analysis and discussion is necessary and will be done in further research, which will concentrate on the use of texture information. In-situ experiments will also be performed to prove the precision and accuracy of classification.

ACKNOWLEDGMENT

2009 Urban Remote Sensing Joint Event

This study was supported by the China Scholarship Council, National Natural Science Foundation of China (Project No. 40771174), Program for New Century Excellent Talents in Universities (Project No. NCET-06-0381), National High Technology Research and Development Program of China (863 Program), (Project No. 2007AA12Z178 and 2009AA12Z131), Key Laboratory of Advanced Engineering Surveying of SBSM (Project No. TJES0810), and grants from the Shanghai ShuGuang Scholarship Program (Project No. 07SG24). We are also very grateful to persons and institutions, which provided accurate and reliable data for the original criteria.

Special thanks are given to the hyperspectral research group at DLR, especially Dr. Andreas Müller and Wieke Heldens, who enabled this work by supplying the hyperspectral data and the DSM free of charge.

REFERENCES

- [1] Acharyya, M., De, R.K. and Kundu, M.K., 2003. Segmentation of remotely sensed images using wavelet features and their evaluation in soft computing framework, *IEEE Transactions on Geoscience and Remote Sensing*, Vol. 41, No. 12, pp. 2900-2905.
- [2] Anderson, J.R., Hardy, E.E., Roach, J.T. and Witmera, R.E., 1976. Land Use And Land Cover Classification System For Use With Remote Sensor Data, U.S. Geological Survey Professional Paper, No. 964. USGS, Washington, D.C.
- [3] Baatz, M., Benz, U., Dehghani, S., Heynen, M., Hltje, A., Hofmann, P., Lingenfelder, Iris., Mimler, M., Weber, M. and Willhauck G., 2004. User Guide of eCognition, Germany, Definiens Imaging GMBH, pp. 110-122.
- [4] Bolstad P. V. and Lillesand T. M., 1991. Rapid maximum likelihood classification, *Photogrammetric Engineering and Remote Sensing*, Vol. 57, No. 1, pp. 64-74.
- [5] Cocks, T., Jenssen, R., Stewart, A., Wilson, I. and Shields, T., 2001. The HymapTM Airborne Hyperspectral Sensor: The System, Calibration and Performance, 1st EARSeL Workshop on Imaging Spectroscopy, edited by Schaeppman ME, Schlpfer D and D Itten K (EARSeL, Paris), pp. 37-42.
- [6] Douglas D.H. and Peucker T. K., 1973. Algorithms for the reduction of the number of points required to represent a line or its caricature. *The Canadian Cartographer*, Vol. 10, No. 2, pp. 112-122.
- [7] Duarte-Carvajalino, J. M., Sapiro, G., Velez-Reyes, M. and Castillo, P. E., 2008. Multiscale Representation and Segmentation of Hyperspectral Imagery Using Geometric Partial Differential Equations and Algebraic Multigrid Methods, *IEEE Transactions on Geoscience and Remote Sensing*, Vol. 46, No. 8, pp. 2418-2434.
- [8] Jia, X. and Richards, J.A., 1993. Binary coding of imaging spectrometer data for fast spectral matching and classification, *Remote Sensing of Environment*, Vol. 43, pp. 47-53.
- [9] Kartikeyan, B., Sarkar, A. and Majumder, K.L., 1998. A segmentation approach to classification of remote sensing imagery, *International Journal of Remote Sensing*, Vol. 19, No.9, pp. 1695-1709.
- [10] Lee, C. and Landgrebe, D.A., 1991. Fast likelihood classification, *IEEE Transactions on Geoscience and Remote Sensing*, Vol. 29, No. 4, pp. 509-517.
- [11] Le Moigne, J. and Tilton, J.C., 1995. Refining image segmentation by integration of edge and region data , *IEEE Transactions on Geoscience and Remote Sensing*, Vol. 33, No. 3, pp. 605-615.
- [12] Mazer, A.S., Martin, M., Lee, M. and Solomon, J.E., 1988. Image processing software for imaging spectrometry data analysis, *Remote Sensing of Environment*, Vol. 24, pp. 201-210.
- [13] Robinson, D.J., Redding, N.J. and Crisp, D.J., 2002. Implementation of a fast algorithm for segmenting SAR imagery, *Scientific and Technical Report*, Australia: Defense Science and Technology Organization.
- [14] Swain, P.H. and Davis S.M., 1978. *Remote Sensing: The Quantitative Approach*. McGraw- Hill, New York, NY, 396p.
- [15] Trias-Sanz, R., Stamon G. and Louchet, J., 2008. Using colour, texture, and hierarchial segmentation for high-resolution remote sensing, *ISPRS Journal of Photogrammetry and remote sensing*, Vol. 63, No. 2, pp. 156-168.
- [16] Viterbi, A. J. and Omura, J. K., 1979. *Principles of Digital Communication and Coding*. McGraw-Hill, New York, NY, pp. 81.